Region Division of DCE-MRI Breast Tumors by Spectral Clustering

Technical Report

Sophie Roscher

Otto-von-Guericke-University Magdeburg
sophie.roscher@st.ovgu.de

Abstract. Diagnosis of breast tumors is not always possible with X-ray mammography. Because of its additional information, dynamic contrast enhanced magnetic resonance imaging (DCE-MRI) can improve classification into benignity or malignancy. In clinical research, the expert evaluates the whole lesion, single voxels, or regions of interest (ROIs). The presented approach focuses on ROI-based evaluation. For generation of ROIs, i.e. groups of homogeneous tumor voxels, a spectral clustering approach is adapted because of its ability to form spatially connected clusters with arbitrary shape. In addition, a set of clustering parameters is derived semi-automatically so that no user input is necessary. Based on the clustering result, features from the most suspect region and the whole tumor are extracted and a decision tree is learned to determine malignancy or benignity of a lesions. A first experiment shows that this approach is able to correctly classify 82.6% instances of the tested data.

1 Introduction

Malignant breast tumors are characterized by a "formation of new vessels and/or the sprouting of existing capillaries in the peritumoral stroma" [Kuh07]. This process is called neoangiogenesis. X-ray mammography is often used for evaluation of breast tumors. However, it is not always possible to make a clear decision. Particularly younger women have dense breast tissue that does not reveal pathologic masses. The additional information of dynamic contrast enhanced magnetic resonance imaging (DCE-MRI) can improve breast tumor evaluation. Because of its high sensitivity it even may reveal yet undetected metastasis. However, DCE-MRI's specificity is only moderate compared to X-ray mammography. To improve the specificity, and therefore the automatic classification of breast lesions, the lesion's heterogeneity and the lesion enhancement kinetics are evaluated in clinical research [GPTP10].
Typically, newly formed vessels of the tumor yield an early contrast agent (CA) enhancement and therefore a strong CA wash-in. In addition, a rapid CA washout is caused by the highly permeable vessels. In current clinical research, radiologists evaluate kinetic CA enhancement based on the whole lesion, single voxels or regions of interest (ROIs). This approach focuses on ROI-based evaluation. Therefore, The ROI's average relative enhancement (RE) over time - the

RE curve - is computed. From the early RE and the curve's shape, the radiologist assesses the CA wash-in and wash-out to distinguish between malignant and benign tumors. The manual selection of the ROI is a very cumbersome and error-prone task. In the study of Chen et al. [CGBN06], a clustering based on fuzzy c-means is applied to automatically identify the most characteristic RE curve from breast lesions. Glaßer et al. [GPTP10] suggest a region merging to create partitions with similar perfusion characteristics and to compute quantitative and qualitative measurements to provide additional information for detecting malignant breast cancer. In their recent work [GNP+13], a density-based clustering followed by a connected component analysis is applied to detect the most suspect region. In a second step, a decision tree is learned based on features of this region to automatically distinguish between benign and malignant tumors.
The grouping of the tumor voxels into homogeneous regions in terms of their perfusion characteristics is a challenging task due to noise of the individual voxels' RE curves. In this study, a spectral clustering based approach is presented that integrates both perfusion characteristics and spatial information for a spatially connected and homogeneous region division. In addition, a set of clustering parameters is proposed based on empirical studies and dynamic computations that analyze the properties of the tumor, so that no user-input is necessary. Based on the resulting partitioning, meaningful features are extracted to learn a decision tree that distinguishes between malignant and benign breast cancer. The approach was evaluated with a data set of 68 breast tumors whose malignancy or benignity could not be clearly diagnosed by X-ray mammography.
Spectral clustering was successfully employed in applications like image segmentation ([SM00], [MBLS01], [ZTW06]), text mining [BJ06] and data mining of large network data sets [WS05]. Compared to simple clustering algorithms like k-means, it is invariant to cluster shapes and densities and does not get stuck in local minima. In recent years, there have been many studies and improvements of spectral clustering. In [AV13], the performance of various proximity measures when applied to spectral clustering algorithms is analyzed. Zelnik-Manor and Perona [ZMP04] propose a system to automatically determine the optimal cluster number and to select an appropriate scale for computing the affinity between each pair of points. A basic comparison of some spectral clustering methods has been proposed in [VM03]. Li et al. [LLCT07] address the problem of robust spectral clustering of data containing significant noise and an unknown number of clusters.

2 Material and Methods

The section gives a detailed description of the medical image data containing breast tumors and outlines the spectral clustering approach to classify lesions into malignant and benign breast cancer.

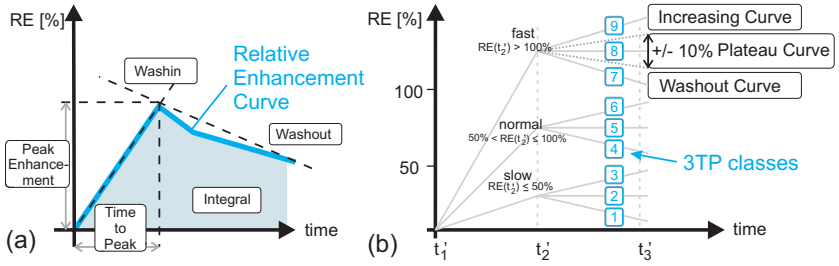

Fig. 1. In (a) an RE curve and its descriptive perfusion parameters are depicted. In (b), the 3TP classes based on RE at t'_1, t'_2, and t'_3 are presented. (Image retrieved from [GNP+13]).

2.1 Tumor Data

The data sets comprise 50 patients with 68 breast tumors. 31 tumors proved to be benign and 37 malignant (confirmation was carried out via histopathologic evaluation or by follow up studies after six to nine months). All lesions could be only detected in DCE-MRI.
The data sets were acquired with an 1.0 T open MR scanner and exhibit the parameters: in-plane resolution $\approx 0.67 \times 0.67 mm^2$, matrix $\approx 528 \times 528$, number of slices ≈ 100, slice gap $= 1.5mm$, number of acquisitions $= 5 - 6$ and total acquisition time $\approx 400s$. During and immediately after the bolus injection of CA, one pre-contrast and four to five post-contrast images were acquired per series. Since DCE-MRI data exhibit motion artifacts mainly due to thorax expansion through breathing and patient's movement, motion correction was carried out with MeVisLab (www.mevislab.de), employing the elastic registration developed by Rueckert et al. [RSH+99]. Next, the relative enhancement (RE) of a tumor, i.e. the percent aged signal intensity increase, is calculated with

$$RE = \frac{(SI_c - SI)}{SI \times 100}$$

[Kuh07]. Here, SI is the pre-contrast and SI_c is the post-contrast signal intensity. Each breast tumor was segmented by an experienced radiologist. The segmentation comprises only voxels exhibiting an RE higher than a predefined threshold at the first time step after the early post-contrast phase [PGP+12].

2.2 Clustering

The RE plotted over time yields RE curves that allow for the extraction of the following descriptive perfusion parameters: wash-in (the steepness of the ascending curve), wash-out (the steepness of the descending curve), integral (the area under the curve) and time to peak (the time when peak enhancement occurs), which are substitutes for physiological parameters like tumor perfusion and vessel permeability (see Figure 1(a)).

Based on these properties, a spectral clustering method is carried out to divide each tumor into homogeneous and spatially continuous clusters. The following paragraph gives a short overview of the basic idea of spectral clustering and specifies the clustering parameters that are used in this approach. A more detailed review of spectral clustering is given in the tutorial of Luxburg et al. [VL07].
The purpose of clustering is to separate data points into several groups such that points in the same group have similar properties and points in different groups are dissimilar to each other. In spectral clustering, this problem is reformulated as a graph cut problem: The data points are considered as nodes of a connected graph and clusters are found by partitioning the graph such that edges between different groups have very low weights and edges within the same cluster have high weights. Such a graph cut can be easily found by using the eigenvectors and eigenvalues of a specific matrix - the Laplacian matrix - to map the original data points in a low dimensional space that can be easily clustered.
The weighted, undirected graph for spectral clustering is constructed from the initial data set whereas each node represents a data point and each edge measures the similarity between two points by some symmetric and non-negative similarity function. Based on this affinity matrix, a Laplacian matrix is constructed and an eigenvalue decomposition is performed. The eigenvalues and eigenvectors are used to map the original data points to a k dimensional subspace - the spectral domain. This new representation should now contain well expressed clusters that can be separated by applying simple clustering techniques like k-means.
In this approach, the breast tumor data sets consist of voxels that are represented as regular data arranged in an orthogonal three dimensional grid. Each voxel includes four descriptive perfusion parameters: wash-in, wash-out, integral and time to peak. This information is normalized and used to construct a similarity graph for the Ng-Jordan-Weiss algorithm [VL07] - a multi-way spectral clustering algorithm - that partitions the data into k groups directly. Each node of the graph represents a voxel of the corresponding breast tumor. To obtain spatially connected clusters, each node is connected to its adjacent nodes in a 26-neighborhood. As proposed in [VL07], the Gaussian similarity function:

$$s(x_i, x_j) = exp(-\frac{dist(x_i, x_j)}{2\sigma^2})$$

is used to represent the local neighborhood relationships. The distance $dist(x_i, x_j)$ between two points is measured by using the cosine similarity of the corresponding perfusion data as proposed in [AV13]. The scaling parameter σ describes how rapidly the affinity decreases with increasing distance between x_i and x_j. Instead of manually selecting σ, a local scaling parameter is calculated for each data point as proposed by Zelnik-Manor et al. [ZMP04]. This parameter depends only on the number of neighbors n that should be considered to compute the scale. An empirical study was employed to find an n that achieves best clustering results for the breast tumor data used here. Therefore, three internal cluster validation measurements [RAAQ11]:

– Davie-Bouldin index,

– Dunn-like index and
– Calinski-Harabasz index

were computed. The validity indices evaluate the resulting cluster in dependence of n: While the number of clusters is fixed, the number of neighbors is varied in the range of $n = \{3, 5, 7, 9, 11\}$ and the cluster results are analyzed. As shown in Figure 2, all three validity indices generally achieve good results for $n = 3$, regardless of the number of clusters. After mapping the initial data to the spectral domain, a k-means clustering is performed. To specify the number of clusters k automatically, several methods have been proposed, e.g. analyzing the eigengap [VL07] or exploiting the structure of the eigenvectors [ZMP04]. Unfortunately, the breast tumor data are noisy, so these methods become less effective (see Figure 3). In this approach, the validity indices, mentioned above, are used to find an optimal k for each data set. Therefore, the spectral clustering algorithm is calculated several times with different cluster numbers ($k = \{3, 4, ..9\}$) and the best k is selected automatically according to the majority of the validation measurements. In case there is no clear decision, a k based on the best (i.e. minimal) Davie-Bouldin index is chosen as suggested in [HBV02].

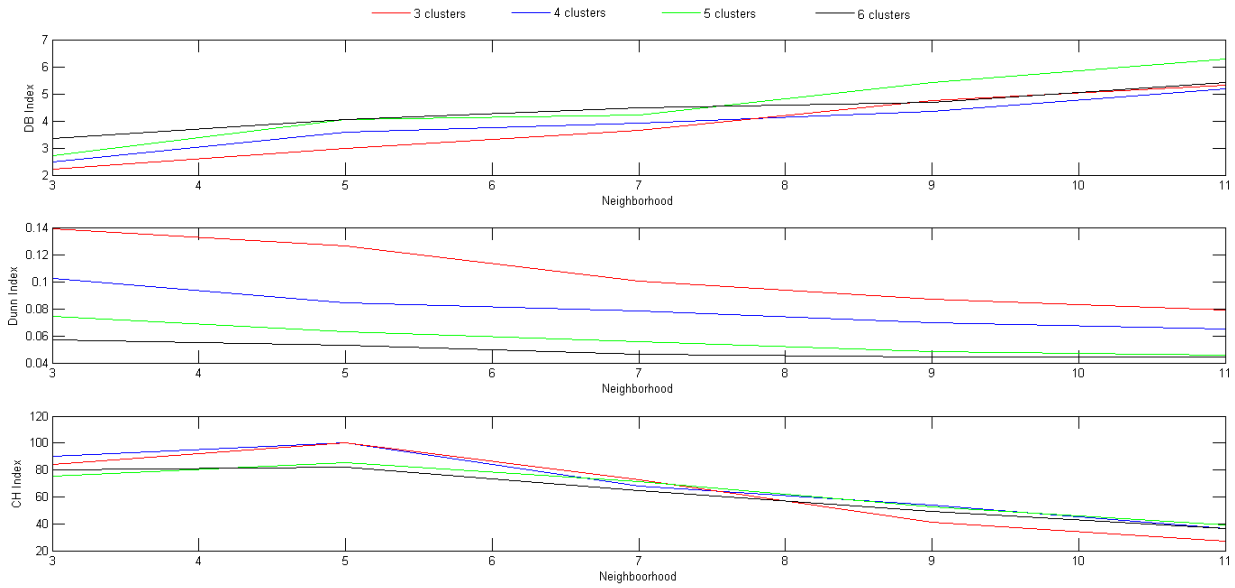

Fig. 2. Result of the average Davie-Bouldin (DB), Dunn-like (Dunn) and Calinski-Harabasz (CH) index for a varying number of neighbors ($n \in \{3, 5, 7, 9, 11\}$) and a fixed cluster number. For $n = 3$, all indices show good results (a minimal DB, a maximal Dunn and a maximal CH index), regardless of the number of clusters.

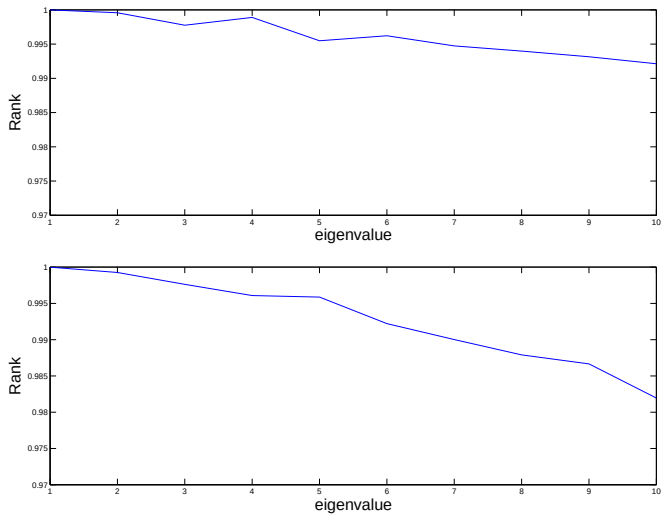

Fig. 3. The eigengap is the difference between two successive eigenvalues. It can be used to estimate the number of clusters in spectral clustering [VL07]. In this approach, the eigengap is not visible due to noise.

2.3 Feature Extraction

Based on the clustering, features are extracted for classification. In the first step, the most suspect region of the clustering result is determined, because a tumor is as malignant as its most malignant part. Therefore, the three-time-point (3TP) method is applied by [DGW+97]. This technique assigns automatically each voxel's RE curve to an 3TP class based on three time points. In this study, the most suspicious region corresponds to the largest cluster with a most frequent RE curve of 3TP class 7. If no such cluster exists, a cluster with the 3TP class 9, 8, 4, 6, 5, 1, 3, 2 in that order is identified as the most suspect one (see Figure 1b). This user-defined ranking is based on definitions of the most malignant tumor enhancement kinetics: a present wash-out in combination with a strong wash-in [GNP+13]. In the next step, both features from the whole tumor as well as from the most suspicious region are extracted (see Table 1). This information is used to learn a classifier that distinguishes between malignant and benign breast cancer. Here, a decision tree model is used because of its simplicity and interpretability. The most important features according to the decision tree are shown in Figure 4.

Abbreviation	Description
3TP class	most frequent 3TP class of most suspect cluster
Rel. size	size of most suspect region in relation to the whole tumor
WI	average wash-in of most suspect region
WO	average wash-out of most suspect region
Integral	average integral of most suspect region
age	age of the patient
#cluster	number of clusters
Hom	average homogeneity (i.e. intra-cluster variance) of the clusters [ZXF09]
Sep	separability (i.e. inter-cluster variance) of the clusters [ZXF09]
P	Purity index*
J	Jaccard index*
F1	F1 score*

*based on the comparison of the clustering result and the 3TP method classification of all tumor voxels

Table 1. List of features that are used to learn a decision tree.

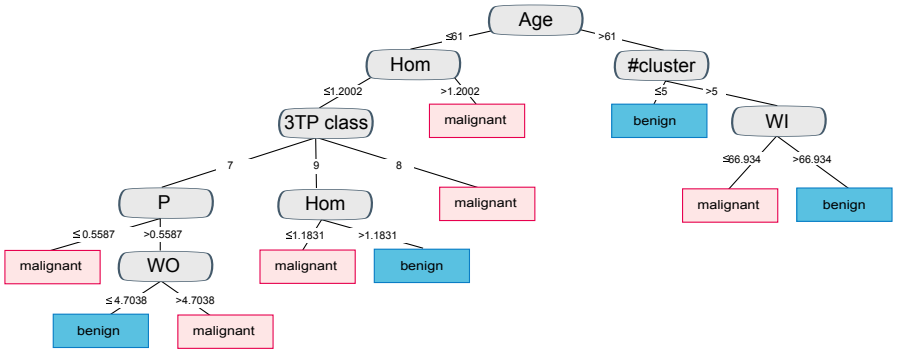

Fig. 4. The learned decision tree is able to correctly classify 82.5% instances of the tested data.

3 Results

The tumor data set used for clustering has no ground truth to evaluate the spectral clustering approach directly. However, the malignancy or benignity of each breast tumor is known and thus, is used for evaluation.
The experiment shows that features extracted from clusters of the spectral clustering are promising. 56 of 68 tumors were classified correctly, i.e. a recall of 82.24% was achieved. By comparison, the recall of the density-based method proposed in [GNP+13] is only 77.9%. Furthermore, the approach of Glaßer et al. does not consider spatial distribution of the data points for clustering. Hence, a post-processing step has to be applied to obtain spatially connected regions that represent homogeneous regions of the tumor, with respect to the perfusion char-

acteristics. However, using a connected component analysis in a post-processing step can lead to very small clusters. In contrast, spectral clustering uses a connectivity graph to integrate spatial information for clustering directly.

4 Discussion

In this paper, a spectral clustering algorithm for partitioning of DCE-MRI breast tumors was adapted. The result of the region division was employed to predict a tumor's malignancy and shows promising results compared to the density-based clustering as proposed in [GNP+13]. By making use of the 26-neighborhood of the data to build a connectivity graph for spectral clustering, there is no need to apply a post-processing step to obtain spatially connected regions. Furthermore, spectral clustering is able to detect clusters with arbitrary shape and does not get stuck in local minima. Despite a difficult data base, see section 2.1, the classification result is promising.
The disadvantages of spectral clustering are its sensitivity to the parameter choice (e.g. cluster number, neighborhood, similarity measure for the adjacency matrix) and a difficult interpretation of the clustering result. In this study, a set of semi-automatically derived parameters was presented to achieve good classification results. For improvement of the clustering process, the k-means approach to construct the final solution in spectral domain can be replaced by a more advanced technique as proposed in [BJ06]. Despite good classification results, the evaluation of the perfusion parameters is difficult. As shown in Figure 5, the features do not seem to be suitable for separation in 1D, i.e. there is no clear distinction between features of malignant and benign tumors visible. A definition of alternate features (e.g. description of cluster shape) could enhance the results.

References

[AV13] Nadia Farhanaz Azam and HernaL. Viktor. Spectral Clustering: An Explorative Study of Proximity Measures. In *Knowledge Discovery, Knowledge Engineering and Knowledge Management*, volume 348 of *Communications in Computer and Information Science*, pages 60–78. Springer Berlin Heidelberg, 2013.

[BJ06] Francis R. Bach and Michael I. Jordan. Learning Spectral Clustering, with Application to Speech Separation. *Journal of Machine Learning Research*, 7:1963–2001, 2006.

[CGBN06] Weijie Chen, Maryellen L Giger, Ulrich Bick, and Gillian M Newstead. Automatic Identification and Classification of Characteristic Kinetic Curves of Breast Lesions on DCE-MRI. *Medical Physics*, 33:2878, 2006.

[DGW+97] Hadassa Degani, Vadim Gusis, Daphna Weinstein, Scott Fields, and Shalom Strano. Mapping Pathophysiological Features of Breast Tumors by MRI at High Spatial Resolution. *Nature medicine*, 3(7):780–782, 1997.

[GNP+13] Sylvia Glaßer, Uli Niemann, Uta Preim, Bernhard Preim, and Myra Spiliopoulou. Classification of Benign and Malignant DCE-MRI Breast Tumors by Analyzing the Most Suspect Region. In *Bildverarbeitung für die Medizin 2013*, pages 45–50. Springer, 2013.

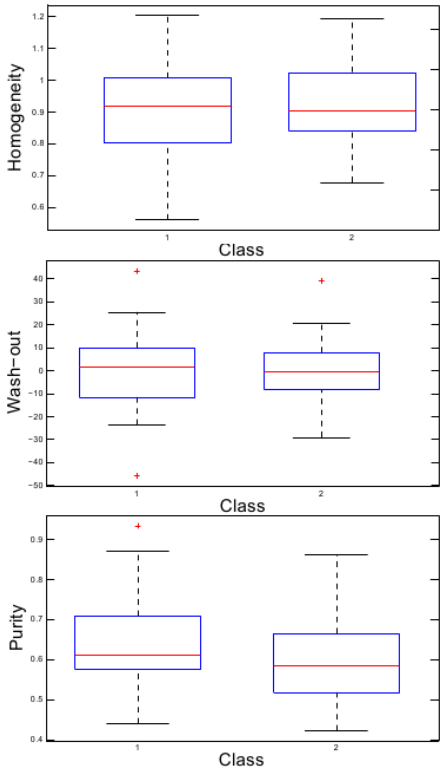

Fig. 5. Box plots of benign (1) and malignant (2) tumor data for homogeneity (top), wash-out (middle) and purity (bottom). Despite good classification results, the chosen features do not seem to be optimal for separation.

[GPTP10] Sylvia Glaßer, Uta Preim, Klaus Tönnies, and Bernhard Preim. A Visual Analytics Approach to Diagnosis of Breast DCE-MRI Data. *Computers & Graphics*, 34(5):602–611, 2010.

[HBV02] Maria Halkidi, Yannis Batistakis, and Michalis Vazirgiannis. Clustering Validity Checking Methods: Part II. *ACM Sigmod Record*, 31(3):19–27, 2002.

[Kuh07] Christiane Kuhl. The Current Status of Breast MR Imaging Part I. Choice of Technique, Image Interpretation, Diagnostic Accuracy, and Transfer to Clinical Practice. *Radiology*, 244(2):356–378, 2007.

[LLCT07] Zhenguo Li, Jianzhuang Liu, Shifeng Chen, and Xiaoou Tang. Noise Robust Spectral Clustering. In *Proc. of IEEE Conference on Computer Vision*, pages 1–8, 2007.

[MBLS01] Jitendra Malik, Serge Belongie, Thomas Leung, and Jianbo Shi. Contour and Texture Analysis for Image Segmentation. *Journal of computer vision*, 43(1):7–27, 2001.

[PGP+12] Uta Preim, Sylvia Glaßer, Bernhard Preim, Frank Fischbach, and Jens Ricke. Computer-aided Diagnosis in Breast DCE-MRI – Quantification

of the Heterogeneity of Breast Lesions. *European Journal of Radiology*, 81(7):1532 – 1538, 2012.

[RAAQ11] Eréndira Rendón, Itzel Abundez, Alejandra Arizmendi, and Elvia M Quiroz. Internal versus External Cluster Validation Indexes. *Journal of computers and communications*, 5(1):27–34, 2011.

[RSH+99] Daniel Rueckert, Luke I Sonoda, Carmel Hayes, Derek LG Hill, Martin O Leach, and David J Hawkes. Nonrigid Registration Using Free-Form Deformations: Application to Breast MR Images. *IEEE Trans Med Imaging*, 18(8):712–21, 1999.

[SM00] Jianbo Shi and Jitendra Malik. Normalized Cuts and Image Segmentation. *IEEE Transactions on Pattern Analysis and Machine Intelligence*, 22(8):888–905, 2000.

[VL07] Ulrike Von Luxburg. A Tutorial on Spectral Clustering. *Statistics and computing*, 17(4):395–416, 2007.

[VM03] Deepak Verma and Marina Meila. A Comparison of Spectral Clustering Algorithms. Technical report, Department of CSE. University of Washington. Seattle, 2003.

[WS05] Scott White and Padhraic Smyth. A Spectral Clustering Approach to Finding Communities in Graphs. In *Proc. of SIAM Conference on Data Mining*, pages 76–84, 2005.

[ZMP04] Lihi Zelnik-Manor and Pietro Perona. Self-tuning Spectral Clustering. In *Proc. of Advances in neural information processing systems*, pages 1601–1608, 2004.

[ZTW06] Ulas Ziyan, David Tuch, and Carl-Fredrik Westin. Segmentation of Thalamic Nuclei from DTI using Spectral Clustering. In *Medical Image Computing and Computer-Assisted Intervention–MICCAI 2006*, pages 807–814. Springer, 2006.

[ZXF09] Qinpei Zhao, Mantao Xu, and Pasi Fränti. Sum-of-squares Based Cluster Validity Index and Significance analysis. In *Adaptive and Natural Computing Algorithms*, pages 313–322. Springer, 2009.